Catechol and Humic Acid Sorption onto a Range of Laboratory-Produced Black Carbons (Biochars)

GABRIEL N. KASOZI,[†]
ANDREW R. ZIMMERMAN,*,[†]
PETER NKEDI-KIZZA,[‡] AND BIN GAO[§]

Department of Geological Sciences, University of Florida, 241 Williamson Hall, Gainesville, Florida 32611-2120, Department of Soil and Water Science, University of Florida, Gainesville, Florida, and Department of Agricultural and Biological Engineering, University of Florida, Gainesville, Florida

Although the major influence of black carbon (BC) on soil and sediment organic contaminant sorption is widely accepted, an understanding of the mechanisms and natural variation in pyrogenic carbon interaction with natural organic matter (NOM) is lacking. The sorption of a phenolic NOM monomer (catechol) and humic acids (HA) onto BC was examined using biochars made from oak, pine, and grass at 250, 400, and 650 °C. Catechol sorption equilibrium occurred after 14 d and was described by a diffusion kinetic model, while HA required only 1 d and followed pseudo-second-order kinetics. Catechol sorption capacity increased with increasing biochar combustion temperature, from pine < oak < grass and from coarse < fine particle size. At lower catechol concentrations, sorption affinity (Freundlich constant, K_f) was directly related to micropore surface area (measured via CO_2 sorptometry) indicating the predominance of specific adsorption. In contrast, HA exhibited an order of magnitude less sorption (0.1% versus 1%, by weight) due to its exclusion from micropores. Greater sorption of both catechol and HA occurred on biochars with nanopores, i.e. biochars made at higher temperatures. These findings suggest that addition of BC to soil, via natural fires or biochar amendments, will sequester abundant native OM through sorption.

Introduction

Black carbon (BC), the residues of incomplete biomass combustion, has received much attention from environmental chemists due to the recent discovery of its widespread distribution in soils and sediments (*1*) and its potential role in controlling the fate and toxicity of many environmental organic contaminants (*2*). In addition, the discovery of small plots of fertile Amazonian soil known as *terra preta*, enriched in BC, nutrients and non-BC natural organic matter (NOM) compared to surrounding native tropical soils has inspired the idea that biochar, BC made by biomass combustion, could be added to soils to increase fertility (*3*). Because biochar is a refractory form of organic C (*4*), it can also enhance soil

C sequestration. Biochar amendments might have an even greater atmospheric CO_2 drawdown effect if NOM sorption and protection occurs. However, understanding of the capacity, mechanisms, and variability in biochar NOM sequestration are currently lacking.

The primary mechanisms by which NOM may be preserved over long time scales in soils and sediment include physical protection within nanopores or other occluding structures and sorptive protection, both of which can shield OM from enzymatic attack. Correspondingly, two fundamental characteristics of BC or biochars that could, potentially, contribute to its ability to sorb and protect (stabilize) NOM include its well-developed pore structure and its highly sorbent surficial chemistry. However, just as BC is actually composed of a range of materials of varying reactivity, or a 'combustion continuum' (*1*), biochar too has been found to vary greatly in surface chemistry and morphology, primarily based upon combustion conditions (*4*).

Previous works contributing to our current understanding of the sorption characteristics of pyrogenic carbons come mainly from two general research areas: 1) examinations of the adsorption of a wide variety of organic compounds onto 'activated' carbons, mainly for industrial and water treatment purposes, and 2) examinations of the interaction of hydrophobic organic chemicals (HOCs) with soil BC and individual biochars for the purpose of understanding contaminant fate and transport. Activated carbons, chars altered with physical or chemical treatment or by heating above 800 °C, possess large surface areas or highly functionalized surfaces, designed to maximize adsorption of target compounds. Thus, they show high adsorption affinity for a wide range of organic components including a variety of phenolic compounds (*5*), halogenated aromatic and polyaromatic hydrocarbons (*6*, *7*), and humic acids (*8*). While both electrostatic and nonelectrostatic interaction mechanisms are considered important in activated carbon adsorption, removal of oxygen-containing functional groups is thought to enhance the sorption of both polar and nonpolar organic compounds from aqueous solution (*6*).

Although NOM distribution has long been known to influence the sorption and, thus, bioavailability of many organic contaminants, more recent work as identified separate geosorbent domains within soils and sediments exhibiting differing sorption behavior. The so-called 'soft' and a 'hard' sorption domains have been proposed to dominate the sorption of neutral organic chemicals in many soils and have been identified as amorphous NOM and carbonaceous sorbents (including BC, coal, and kerogen), respectively (e.g. refs *9* and *10*). Compared to NOM whose sorption of neutral organic chemicals tends to be concentration dependent and yields linear isotherms, BC sorption isotherms tend to be nonlinear (*2, 11*), possibly as a result of BC's heterogeneous surface. In addition, BC has been reported to have an order of magnitude or greater sorption capacity than NOM for HOCs (*2, 11−14*) including polycyclic aromatic hydrocarbons and polychlorinated biphenyls (*2, 11, 15*). Thus, BC is thought to be the predominant sorption domain in many soils and sediments.

The nature of the interaction between HOCs and BC is still not fully understood. Unlike the partition model (for NOM) which assumes noncompetitive and homogeneous surface interactions, nonlinear sorption exhibited by BC has been explained by mechanisms such as physical entrapment within micro- and nanopores or BC sheet structures (*10, 16*). Evidence for this can be found in the rate-limited or nonequilibrium nature of HOC-BC interaction (*14, 17*) and

* Corresponding author phone: (352)392-0070; fax: (352)392-9294; e-mail: azimmer@ufl.edu.
† Department of Geological Sciences.
‡ Department of Soil and Water Science.
§ Department of Agricultural and Biological Engineering.

the correspondence between compound planarity and sorption capacity (13, 18, 19). However, chemical adsorption has also been suggested by surface area-HOC sorption correlations and the involvement of $\pi-\pi$ and other specific electron donor and acceptor interactions (18, 19).

While the interactions of mainly HOCs and BC, particularly soot, have been examined, those of NOM with native chars have been far less studied. However, a number of studies have been noted that the presence of NOM causes reductions in HOC sorption affinity on activated carbons (e.g. refs 8, 20, and 21) and natural BC materials (22). In addition, BC added to soil has been noted to sorb less organic contaminants than BC alone (e.g. refs 22 and 23). Both pore blockage and competitive adsorption have been proposed as explanations, supported by the fact that both NOM type and molecular size may influence the amount of sorption inhibition observed (8, 21). It is unclear, however, how variations in biochar type may influence NOM sorption.

This study used batch sorption experiments to examine the kinetics and thermodynamics of catechol and humic acid (HA) sorption on a range of biochars prepared from different biomass types and under a range of combustion conditions. Catechol (1,2-dihydroxybenzene) is a small phenolic compound and is ubiquitously distributed in soil, representing up to 10% of the total dissolved organic carbon (24). Catechol served here as a model HA monomer as phenols, together with carboxylic acids, are regarded as major components of and precursors to humic substances (25). With a $\log(K_{ow})$ of 0.89 (26), catechol is much more hydrophilic than the organic compounds whose sorption to BC have been well-studied. In addition, phenols, and specifically catechol, are widespread environmental contaminants, widely used in cosmetic, pharmaceutical, dye, antiseptics, and petrochemical industries, and are designated priority pollutants by the U.S. Environmental Protection Agency (27).

The goal of this study was to better understand the degree and mechanism by which biochar additions to soil may sequester and protect non-BC OM from degradation and also to explore whether pyrolyzed waste biomass (biochar) might be used as a low cost alternative (to activated carbon) for environmental remediation or wastewater treatment.

Experimental Section

Materials. Biochar was made from representatives of three biomass types: a hard wood (Laurel oak, *Quercus laurifolia*: Oak), a softwood (Loblolly pine, *Pinus taeda*: Pine), and a grass (Eastern gamma-grass, *Tripsacum dacttyloides*: Grass), all collected from north central Florida. The biomass was dried for at least 5 d at 60 °C and cut into 5 cm² pieces. Each biomass type was charred under three conditions: in an oven under full atmosphere at 250 °C and in a pyrolyzer under a stream of N_2 at 400 and 650 °C (notated 250, 400, and 650, respectively). The pyrolyzer was heated at a rate of 26 °C min^{-1} and held at the set temperature for 3 h. Following charring, samples were ground lightly and sieved, yielding fine (<0.25 mm: fn) and coarse (0.25−2 mm: cs) size fraction, which were rinsed thoroughly with distilled water to remove ash and dried at 60 °C for at least 5 d. Subsamples of the coarse biochar were batch leached in distilled water to simulate aging that might occur in the environment. Samples of biochar (10 g) in 250 mL deionized water (Milli-Q, Millipore) were placed in the dark on a shaking table (150 rpm) for 100 days, during which, the supernatant was replaced with water eight times to enhance leaching. Methods used to determine biochar volatile matter (VM%), inorganic content (Ash%), and major element composition are described in detail elsewhere (4). Measurement of surface area including nanopores >1 nm (by N_2 sorptometry: SA-N_2) and micropores <1 nm (by CO_2 sorptometry: SA-CO_2) is described in the Supporting Information provided.

Catechol (>99% purity) was obtained from Acros Organics (New Jersey, U.S.A.) and technical grade HA from Sigma-Aldrich Co. (St. Louis, MO). Stock solutions were prepared in aqueous (Milli-Q, Millipore) 0.01 M CaCl$_2$ and were stored in the dark. This terrestrial peat HA has previously been determined to have the C:H:N:O composition of 56:4.6:0.6:39 weight% and average molecular weight of about 3900 ± 300 Da (28).

Catechol Sorption Experiments. Catechol-biochar sorption kinetics experiments were carried out in triplicate to determine the time period required to reach equilibrium. Amount sorbed onto about 20 mg biochar, determined as the difference between starting (150 mg/L catechol) and final sorbate concentration, was measured over the course of 24 d. Batch mode sorption equilibrium experiments were then carried out in triplicate for each sorbent-adsorbate pair using between 20−100 mg biochar (determined by preliminary experiments to yield detectable sorption levels) weighed into 15 mL glass centrifuge tubes, to which, 10 mL of 6−400 mg L^{-1} catechol solution prepared in 0.01 M aqueous CaCl$_2$ was added. The mixture was allowed to equilibrate in the dark for 14 d on an orbital shaker, after which, the samples were centrifuged 5 min at 4000 rpm and filtered through Whatman# 42 filter paper.

A 20 μL aliquot of filtrate was analyzed for catechol on a Shimadzu HPLC system equipped with a UV/vis detector set to 220 nm, autosampler and 150 × 4 mm Thermo Scientific HyperSil Gold C18 column. Using a 10% acetonitrile (HPLC-grade) mobile phase (1 mL min^{-1}), separation between catechol and biochar leachate was achieved. The calibration curves were linear with $R^2 > 0.98$.

Humic Acids Sorption Experiments. Humic acid (HA) sorption experiments were carried out on 50 mg biochar samples in duplicate 50 mL solutions (0, 3.2, 6.4, 9.6, and 12.8 mg L^{-1} HA in 0.01 M CaCl$_2$) from 20 mg L^{-1} 0.45 μm filtered stock solutions adjusted to pH = 7 using 0.1 M HCl. After the sorption equilibrium period of 3 d on a shaker in the dark, the mixtures were centrifuged 5 min at 4000 rpm, and HA in the supernatants were measured by UV absorption on a Themo Scientific Evolution 300 spectrophotometer set at 254 nm. To reduce the interference from biochar leachate, HA sorption experiments were only carried out using preleached (aged) biochar samples. Also, control treatments with biochar only were included in the experiments, and these were used to correct for the leachate background, which were equivalent to 0.3 mg L^{-1} HA at most.

Data Modeling. Attempts were made to fit the kinetic and equilibrium catechol and HA sorption isotherm data to a number of well-known models to better understand the processes governing catechol and HA sorption to biochars. Details of all models examined and their results are presented in the Supporting Information but only that of the best-fitting models are presented below. Catechol sorption kinetics data was modeled using the intraparticle diffusion equation (Weber-Morris equation) adapted from ref (29)

$$S_t = k_i t^{1/2} + C \qquad (1)$$

where S_t is the sorbed concentration at any time, t, k_i is the apparent diffusion rate constant (mg kg^{-1} d$^{-1/2}$), and C is a constant (mg kg^{-1}). Sorption isotherms data were best simulated using the Freundlich model

$$S_e = K_f C_e^n \qquad (2)$$

where S_e is the equilibrium sorbed concentration (mg kg^{-1}), C_e is the equilibrium sorbate concentration (mg L^{-1}), K_f is the Freundlich affinity coefficient (mg$^{(1-n)}$ L^n kg^{-1}), and n is the Freundlich linearity or 'heterogeneity' parameter.
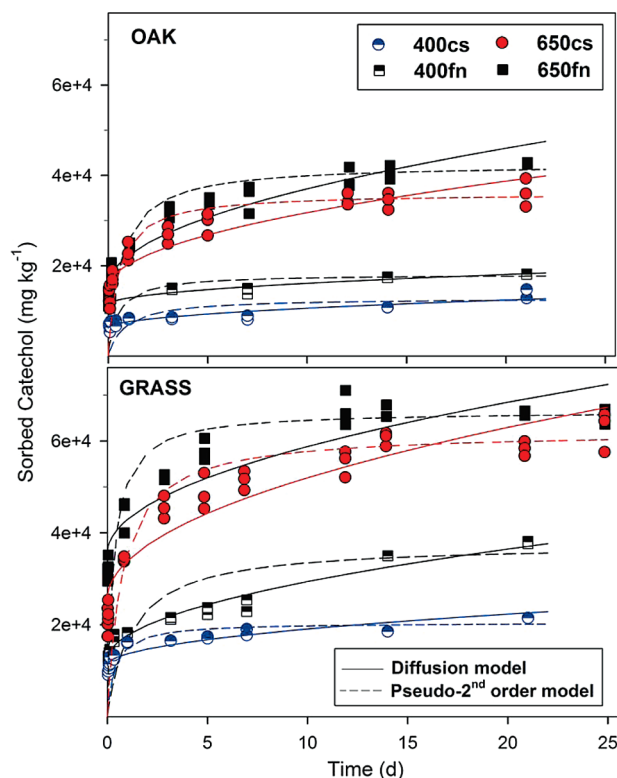
FIGURE 1. Adsorption kinetics data and modeling for catechol onto fine (fn) and coarse (cs) biochar made from oak and grass pyrolyzed at 400 and 650 °C.

Results and Discussions

Sorbent Properties. Differences in biochar characteristics with production temperature were more dramatic than with biomass type (Supporting Information Table S1). Percent organic carbon content (C%) ranged 53−83% and increased with increasing pyrolysis temperature due to progressive loss of H and O-containing functional groups, reflecting dehydration and decarboxylation reactions (30). Generally decreasing VM% and increasing Ash% and surface area with increasing pyrolysis temperature reflect progressive loss of more volatile organic components primarily occurring within or otherwise blocking both nano- and micropores made up of a lattice of nonvolatile C-rich material. Supporting this interpretation, both NMR and FT-IR spectroscopic studies have detected the disappearance of aliphatic C (volatile) and increases in aromatic C and O-aryl C (relatively nonvolatile) with increased biomass pyrolysis temperature (30).

SA-N_2 data indicated little surface in the nanopore range (>1 nm) for the low temperature chars (250 and 400 °C), but a significant amount for 650-coarse oak, pine, and grass biochar (225, 285, and 77 $m^2 g^{-1}$, respectively) and 650-aged biochar (166, 59, and 261 $m^2 g^{-1}$, respectively: Table S1). SA-CO_2 was significantly greater in all cases, ranging 164−643 $m^2 g^{-1}$. The surfaces of all biochars were primarily within micropores and that of low temperature biochars were almost completely within micropores. There was no consistent effect of biochar particle size on its surface area.

Catechol Sorption Kinetics. Time-course sorption experiments indicated that, on average, 59 ± 8% (mean ± standard deviation) of the maximum observed catechol sorption onto all biochars was achieved within an initial fast phase of a few days, followed by a slower sorption phase (Figure 1). Of the total catechol sorption observed after 21 d, 69 ± 8% was recorded after only 3 d and 93 ± 6% after 14 d, on average. A 14 d period was, therefore, judged sufficient to establish sorption pseudoequilibrium, and this period was used during further experimentation. These sorption rates

were similar to other findings. The great majority of phenyl urea (19) and PAH compound sorption (13) onto diesel soot occurred within 14 d. They contrast, however, with other previous work that has used equilibration periods of two days or less to generate HOC-BC and activated carbon sorption isotherms (31, 32) and use of a first-order kinetics model to describe sorption of phenol onto activated carbon and a chemically treated wood charcoal (33).

Among the three kinetic models tested, the diffusion model fit the data best with coefficients of determination (R^2) averaging 0.89 ± 0.04 and containing no systematic structure in the plots of residuals. Though 20% greater catechol sorption occurred onto fine- versus coarse-sized biochar particles after 21 days, sorption onto fine particles did not approach equilibrium significantly faster than onto coarse particles, with 60 ± 12% and 58 ± 5% of the maximum observed catechol sorption achieved within 1 d, respectively. These observations suggest that the kinetic limitation of diffusion into the interior of biochar particles occurred during the slow, rather than fast sorption phase. Considering the extended period required to achieve pseudoequilibrium and the micropore dominated structure of the biochars, it is perhaps not surprising that catechol sorption to biochar was controlled by a diffusion-related mechanism. Intraparticle diffusion has been suggested by previous studies as a dominant mechanism accounting for sorption nonequilibrium of HOCs on carbonaceous matter of many types (10, 34). However, it is also possible that a process more akin to absorption or partitioning into the biochar's volatile pore-filling component is responsible for the retardation of catechol uptake.

Catechol Equilibrium Sorption Isotherms. Sorption isotherms were constructed for each biochar type from batch sorption experiments carried out at circum-neutral conditions (pH of 5.5−7.5) at which catechol is expected to be predominantly a neutral species (catechol pK_a = 9.5 (26)). In general, replication was good, with the relative percent standard deviation less than 5%, though those biochars prepared at 250 °C often showed relatively poorer data replication. A number of trends are clear from representative isotherms (Figure 2). Maximum observed catechol sorption increased with combustion temperature for oak and grass biochar within coarse, fine, and aged treatment types. Pine biochars, however, did not clearly follow this trend, with all coarse biochars displaying similar amounts of catechol sorption. While the 250 °C biochars all sorbed catechol to a similar degree, maximum catechol sorption onto 400 and 650 °C biochars increased from pine < oak < grass. Fine-sized biochar consistently sorbed more catechol than the coarse particles, but the amount of increase varied from nonsignificant (in pine) to nearly double for Oak-650. Aged 250 °C biochar sorbed more or similar amounts of catechol than nonaged 250 °C biochar, but aged 400 and 650 °C biochar consistently sorbed less. Interpretation of biochar sorption trends are aided by sorption isotherm modeling.

Catechol Sorption Isotherm Modeling. Among the four isotherm models tested, the Freundlich, Langmuir−Freundlich hybrid, and Toth models performed equally well (average R^2 = 0.91, 0.92, 0.86, respectively: Tables 1, S2, S3, S4, S5 and Figure S8), while the Langmuir model fit was significantly poorer (average R^2 = 0.69). The former three models are commonly used in cases of heterogeneous sorbents, while the latter presumes monolayer coverage and no sorbate intermolecular interaction. The Freundlich model was chosen for focus here as it requires fewer fitting parameters and its output is easier to interpret than that of the other models. In addition, the Freundlich model has been more commonly used to describe sorption of phenols onto activated carbons (e.g. ref (31)) and HA onto black carbons (e.g. refs 22 and 35).
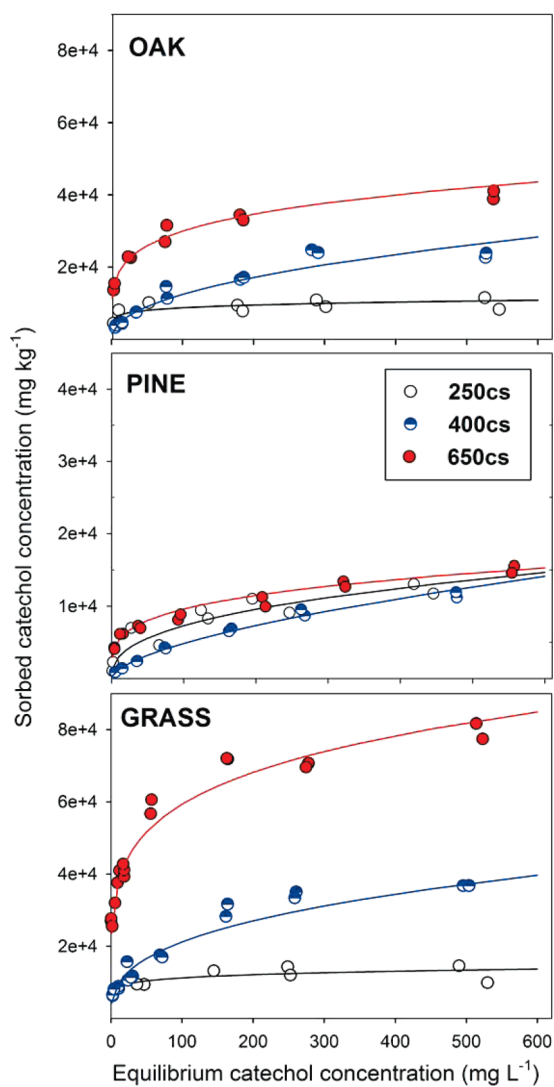
FIGURE 2. Catechol sorption isotherms for coarse-sized oak, pine, and grass biochars. Data modeled using Freundlich model (solid lines). Note *y*-axis scale differs for pine.

For all catechol-biochar isotherms, the Freundlich constants, K_f or 'affinity coefficients', ranged 10^2–10^4 mg^{1-n} L^n kg^{-1}, while those of the Freundlich linearity parameter, n, ranged 0.11–0.63 (0.33 ± 0.16, Table 1, Figure S9). Both higher and lower n values have been recorded for sorption of different phenolic compounds onto activated carbons (*31, 36*). A similar range of both n and K_f have also been reported for more hydrophobic halogenated and PAH compounds sorbed onto carbonaceous materials such as coal, charcoal, and coke (*37, 38*). While all the biochars can, therefore, be considered moderately strong and highly nonlinear sorbents of catechol, there were clear trends among the biochar types. For example, K_f varied consistently with biochar production temperature: 400 < 250 < 650 °C, with parent biomass type: pine < oak < grass, with grain size: coarse < fine, and with treatment: aged < non-aged. However, n generally varied differently with temperature: 250 ≤ 650 < 400 °C, with biomass type: oak ≈ grass < pine, and inconsistently with grain size and treatment. The relatively poorer fit of all the isotherm models for biochars made at 250 °C (Table S3) further suggests the heterogeneity of binding sites on low temperature biochar surfaces and might be attributed to the greater amounts of heteroatoms or volatile matter present on these biochars' surfaces.

To directly compare the sorption affinity of each biochar at specific solution concentrations, a sorption coefficient

solid-water distribution ratio, K_d (in units of L kg^{-1}), was calculated as

$$K_d = \frac{S_e}{C_e} = K_f C_e^{n-1} \qquad (3)$$

The K_d calculated at a sorbate concentration of 1 mg L^{-1} ($K_{d(1)}$), numerically equivalent to K_f, at an upper-end common soil phenol concentration of 20 mg L^{-1} ($K_{d(20)}$ (*24*)), and at half the solubility of catechol ($K_{d(sol/2)}$ at 2.2×10^5 mg L^{-1}) are given in Table 1. Much as for $K_{d(1)}$, $K_{d(20)}$ values were 4–5 times greater for high versus low temperature biochars and the catechol affinity of fine biochars were about twice that of coarse biochar. In contrast, $K_{d(sol/2)}$ was greatest for 400 °C biochars, followed by 650 then 250 °C biochar, suggesting a different sorption mechanism at higher sorbate concentrations.

Within individual biomass types, K_f and $K_{d(20)}$ were most strongly correlated to SA-CO$_2$ ($R^2 = 0.90$ for oak, for example) and indirectly to VM% ($R^2 = 0.73$), implying that surface area, particularly that found in micropores, was most important to catechol sorption and the volatile matter progressively lost at higher combustion temperatures impeded its adsorption by filling pore openings. Aging did not remove this volatile matter as is apparent from the lack of significant change in VM%, SA-CO$_2$ or n after leaching. However, some component of the biochars were removed that may have had affinity for catechol as K_f generally decreased after aging. Alternatively, water may have penetrated the chars during aging and blocked potential catechol bonding sites. However, none of these trends in K_f or $K_{d(20)}$ applied to $K_{d(sol/2)}$ or pine biochar. The former may be explained by a greater importance of partitioning processes at higher solute concentrations and the latter by the overall lower catechol affinity of pine wood biochar. Further understanding of the relative importance of biochar sorption mechanisms may be had through comparison of catechol sorption to that of a large molecular-sized phenolic polymer, i.e. humic acid.

Humic Acid Sorption. Although HA sorption was examined on only aged biochar types because of the interfering NOM released by fresh biochars, some trends were easily discerned. Sorption equilibrium was reached much more quickly than for catechol, with at least 82% of the maximum observed sorption occurring within the first 12 h (Figure 3a). Sorption followed a pseudo-second-order kinetic model indicating that chemical adsorption and not intraparticle diffusion might be the rate-limiting step. In both sorption kinetic and equilibrium sorption experiments, similar HA loading was observed for Oak-400, Grass-400, and Oak-650 biochar, while significantly greater loading and slower kinetics was observed for Grass-650 biochar.

The Freundlich model sufficiently represented all HA-biochar sorption isotherms (Figure 3b). The sorption affinity (K_f) of HA for the 400 °C biochars were about twice that of catechol (Table 1). However, the K_f of Oak-650 and Grass-650, the two aged biochars with considerable nanopore surface area, were 3 and 5 times less than that of catechol for their respective biochars. These observations are consistent with the interpretation that, while HA strongly sorbs to biochar surfaces, likely due to hydrophobic or van der Waals interactions, HA sorption was limited by its exclusion from micropores that were accessible to catechol. However, at least some sorption of HA within biochar nanopore surfaces, when present, is indicated. The mostly greater Freundlich heterogeneity index, n, for HA compared to catechol sorption may indicate a decreased interaction of the polymer with the heterogeneous biochar morphology or chemistry. However, it is also possible that the chemical heterogeneity of the HA, itself, may have led to some of the kinetic and equilibrium sorption characteristics observed.

TABLE 1. Freundlich Model Parameters for Catechol and Humic Acid Sorption to Biochar[a]

	catechol					humic acid		
	K_f	n	R^2	$K_{d,c=20}$	$K_{d(sol/2)}$	K_f	n	R^2
				Coarse Biochar				
Oak-250cs	5014	0.12	0.49	359	0.102	n.d.	n.d.	n.d.
Oak-400cs	1495	0.46	0.92	297	1.973	n.d.	n.d.	n.d.
Oak-650cs	11384	0.21	0.97	1068	0.698	n.d.	n.d.	n.d.
Pine-250cs	1212	0.39	0.86	201	0.766	n.d.	n.d.	n.d.
Pine-400cs	305	0.60	0.99	92	2.245	n.d.	n.d.	n.d.
Pine-650cs	2901	0.26	0.95	309	0.267	n.d.	n.d.	n.d.
Grass-250cs	6768	0.11	0.31	471	0.122	n.d.	n.d.	n.d.
Grass-400cs	4230	0.35	0.95	604	1.446	n.d.	n.d.	n.d.
Grass-650cs	23624	0.20	0.94	2150	1.281	n.d.	n.d.	n.d.
				Coarse-Aged Biochar				
Oak-250a	3498	0.25	0.96	370	0.350	n.d.	n.d.	n.d.
Oak-400a	829	0.52	0.98	197	2.285	1327	0.69	0.99
Oak-650a	6438	0.27	0.89	730	0.914	1957	0.53	0.93
Pine-250a	4722	0.26	0.98	514	0.535	n.d.	n.d.	n.d.
Pine-400a	287	0.61	0.96	89	2.390	n.d.	n.d.	n.d.
Pine-650a	3165	0.28	0.97	366	0.458	n.d.	n.d.	n.d.
Grass-250a	6311	0.14	0.95	480	0.164	n.d.	n.d.	n.d.
Grass-400a	645	0.57	1.00	178	3.288	1555	0.57	0.96
Grass-650a	19149	0.19	0.99	1692	0.918	3464	0.42	0.94
				Fine Biochar				
Oak-250fn	2208	0.35	0.78	315	0.755	n.d.	n.d.	n.d.
Oak-400fn	3229	0.37	0.98	489	1.411	n.d.	n.d.	n.d.
Oak-650fn	10405	0.30	0.97	1278	1.925	n.d.	n.d.	n.d.
Pine-250fn	2322	0.29	0.97	277	0.380	n.d.	n.d.	n.d.
Pine-400fn	334	0.63	0.99	110	3.550	n.d.	n.d.	n.d.
Pine-650fn	6634	0.21	0.98	622	0.407	n.d.	n.d.	n.d.

[a] K_f = Freundlich coefficient (mg^{1-n} L^n kg^{-1}), n = surface heterogeneity index, K_d = Sorption coefficient (L kg^{-1}), R^2 = coefficient of determination, and n.d. = not determined.
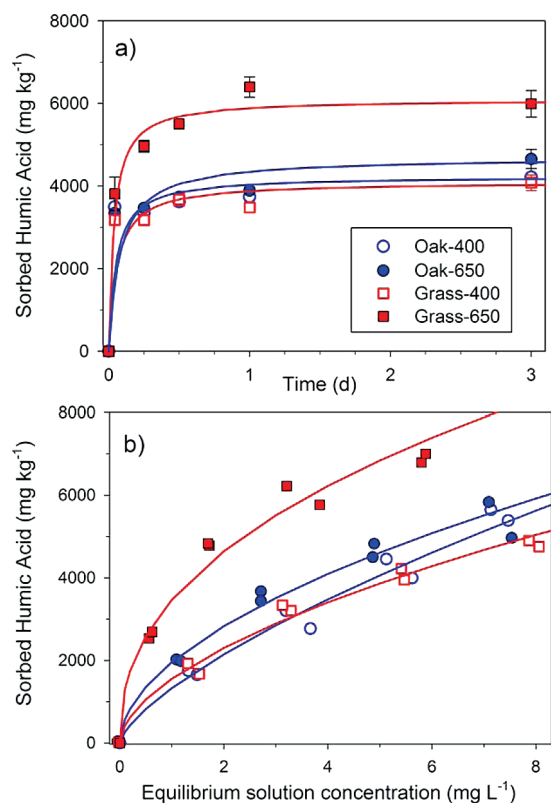
FIGURE 3. Humic acid sorption onto coarse, aged biochar (Oak and Grass, 400 and 650 °C): a) sorption kinetics with pseudo-second-order models and b) sorption isotherms with Freundlich models.

Biochar Sorption Mechanism and Environmental Implications. The concave-downward isotherm shape at low solute concentrations, along with the strong correlation between catechol sorption affinity and micropore surface area (for each biomass type), indicate the dominance of a surface coverage adsorption process for catechol-biochar interaction. Specific electron donor−acceptor interactions have been suggested for other polar compounds with BC such as the adsorption of polar phenyl urea herbicides onto diesel soot (19), napthol onto orange peel chars (39), and nitrobenzene onto wheat residue biochar (40). The lack of linear correlation between SA-CO_2 and catechol sorption across all biochar types, however, indicates that biochar adsorption site density or the chemical nature of the specific interaction may vary with parent biomass type. For example, no physical factor can be found to explain the relatively higher sorption capacity of grass biochar for catechol and HA. However, significant inverse relationships between n and catechol sorption affinity at low ($K_{d(1)}$, $R^2 = 0.78$, Figure S10) and moderate ($K_{d(20)}$, $R^2 = 0.50$) solute concentrations were observed across all biochar samples. This relationship has been noted within other BC sample sets (e.g. refs 37 and 41) and indicates that more heterogeneous sorbents tend to have stronger adsorption components and thus, more nonlinear isotherms. Interestingly, the four samples with the highest SA-N_2 (greatest nanopore component) had much greater sorption affinity than the n versus $K_{d(1)}$ relationship would predict. This suggests that, after uptake of catechol into micropores via pore-filling, further sorption can take place within nanopores, when present, perhaps through capillary condensation, which has been described as an additional adsorptive domain in other biochar sorption studies (e.g. refs 42 and 43).

A number of biochar sorption studies (19, 39, 40) as well as some examining natural BC materials (e.g. refs 37 and 44)

assign an additional role to a partitioning or absorption mechanisms, particular for low temperatures biochars with greater VM% or at higher sorbate concentrations. This may also be the case for catechol whose biochar sorption isotherms become highly linear at higher concentrations. Further, sorption affinity at higher catechol concentrations ($K_{d(sol/2)}$) was not correlated to either SA-CO$_2$ or SA-N$_2$. The positive linear relationship found between n and $K_{d(sol/2)}$ (R^2 = 0.87, Figure S11) suggests that partitioning is of greater influence for more chemically or morphologically homogeneous biochars, i.e. those with VM organic coatings or sorbed OM coatings. Variation in the importance of each of these sorption mechanisms is illustrated in the comparison between 250 and 400 °C biochar. The former was more heterogeneous and of greater sorption affinity at low solute concentrations, while the latter, though of lower surface area, displayed greater sorption affinity and overall sorption capacity at higher solute concentrations due to partitioning into VM.

These findings indicate that biochar in soil might be expected to sorb about 1% of its weight in phenol-like low molecular weight OM or about 0.1% in NOM, depending mainly upon its micropore surface area which, itself, varies mainly with biochar combustion conditions. Parent biomass type and grain size play subdominant roles. Though leaching or degradation of biochar volatile matter might open additional pore surfaces for further adsorption given enough time, adsorption or absorption of large molecular weight NOM to biochar is likely to occur first, thus, blocking pore entrances and allowing only slow sorption into biochar interior surfaces over time. Similarly, HA has been found to attenuate the sorption of organic contaminants onto charcoals (e.g. refs 35 and 45) and activated carbons (20) via pore blocking or competitive adsorption. In either case, biochar soil amendments are likely to enhance long-term soil C sequestration (biochar C and sorbed C) and enhance soil fertility by providing a chemically and morphology complex surface for NOM and nutrient exchange and microbial habitation, much as does soil humic substances. In addition, biochar may find use as a low-cost supersorbent for water treatment or organic contaminant remediation.

Acknowledgments

Supporting Information Available

Additional details on all isotherm models examined, statistical tests used to evaluate their success, tabulated results, example chromatograms and UV spectra, and all isotherms generated. This material is available free of charge via the Internet at http://pubs.acs.org.

Literature Cited

(1) Masiello, C. A. New directions in black carbon organic geochemistry. *Mar. Chem.* **2004**, *92* (1−4), 201–213.

(2) Cornelissen, G.; Gustafsson, O. Effects of added PAHs and precipitated humic acid coatings on phenanthrene sorption to environmental Black carbon. *Environ. Pollut.* **2006**, *141* (3), 526–531.

(3) Lehmann, J.; Joseph, S. Biochar for Environmental Management - An Introduction. In *Biochar for Environmental Management: Science and Technology*; Earthscan: London, UK, 2009; pp 1−12.

(4) Zimmerman, A. R. Abiotic and microbial oxidation of laboratory-produced black carbon (biochar). *Environ. Sci. Technol.* **2010**, *44* (4), 1295–1301.

(5) Liao, Q.; Sun, J.; Gao, L. The adsorption of resorcinol from water using multi-walled carbon nanotubes. *Colloid Surf., A* **2008**, *312* (2−3), 160–165.

(6) Li, L.; Quinlivan, P. A.; Knappe, D. R. U. Effects of activated carbon surface chemistry and pore structure on the adsorption of organic contaminants from aqueous solution. *Carbon* **2002**, *40* (12), 2085–2100.

(7) Guo, Y.; Kaplan, S.; Karanfil, T. The significance of physical factors on the adsorption of polyaromatic compounds by activated carbons. *Carbon* **2008**, *46* (14), 1885–1891.

(8) Li, Q.; Snoeyink, V. L.; Mariaas, B. J.; Campos, C. Elucidating competitive adsorption mechanisms of atrazine and NOM using model compounds. *Water Res.* **2003**, *37* (4), 773–784.

(9) Gustafsson, O.; Haghseta, F.; Chan, C.; MacFarlane, J.; Gschwend, P. M. Quantification of the dilute sedimentary soot phase: Implications for PAH speciation and bioavailability. *Environ. Sci. Technol.* **1997**, *31* (1), 203–209.

(10) Pignatello, J. J.; Xing, B. Mechanisms of slow sorption of organic chemicals to natural particles. *Environ. Sci. Technol.* **1996**, *30* (1), 1–11.

(11) Cornelissen, G.; Breedveld, G. D.; Kalaitzidis, S.; Christanis, K.; Kibsgaard, A.; Oen, A. M. P. Strong sorption of native PAHs to pyrogenic and unburned carbonaceous geosorbents in sediments. *Environ. Sci. Technol.* **2006**, *40* (4), 1197–1203.

(12) Nguyen, T. H.; Sabbah, I.; Ball, W. P. Sorption nonlinearity for organic contaminants with diesel soot: method development and isotherm interpretation. *Environ. Sci. Technol.* **2004**, *38* (13), 3595–3603.

(13) Bucheli, T. D.; Gustafsson, O. Quantification of the soot-water distribution coefficient of PAHs provides mechanistic basis for enhanced sorption observations. *Environ. Sci. Technol.* **2000**, *34* (24), 5144–5151.

(14) Huang, W.; Ping, P.; Yu, Z.; Fu, J. Effects of organic matter heterogeneity on sorption and desorption of organic contaminants by soils and sediments. *Appl. Geochem.* **2003**, *18* (7), 955–972.

(15) Lohmann, R.; MacFarlane, J. K.; Gschwend, P. M. Importance of black carbon to sorption of native PAHs, PCBs, and PCDDs in Boston and New York, Harbor sediments. *Environ. Sci. Technol.* **2005**, *39* (1), 141–148.

(16) Golding, C. J.; Smernik, R. J.; Birch, G. F. Investigation of the role of structural domains identified in sedimentary organic matter in the sorption of hydrophobic organic compounds. *Environ. Sci. Technol.* **2005**, *39* (11), 3925–3932.

(17) Brusseau, M. L.; Rao, P. S. C. The influence of sorbate-organic matter interactions on sorption nonequilibrium. *Chemosphere* **1989**, *18* (9−10), 1691–1706.

(18) Jonker, M. T. O.; Koelmans, A. A. Sorption of polycyclic aromatic hydrocarbons and polychlorinated biphenyls to soot and soot-like materials in the aqueous environment: mechanistic considerations. *Environ. Sci. Technol.* **2002**, *36* (17), 3725–3734.

(19) Sobek, A.; Stamm, N.; Bucheli, T. D. Sorption of phenyl urea herbicides to black carbon. *Environ. Sci. Technol.* **2009**, *43* (21), 8147–8152.

(20) Guo, Y.; Yadav, A.; Karanfil, T. Approaches to mitigate the impact of dissolved organic matter on the adsorption of synthetic organic contaminants by porous carbonaceous sorbents. *Environ. Sci. Technol.* **2007**, *41* (22), 7888–7894.

(21) Pelekani, C.; Snoeyink, V. L. Competitive adsorption between atrazine and methylene blue on activated carbon: the importance of pore size distribution. *Carbon* **2000**, *38* (10), 1423–1436.

(22) Cornelissen, G.; Gustafsson, O. Sorption of phenanthrene to environmental black carbon in sediment with and without organic matter and native sorbates. *Environ. Sci. Technol.* **2004**, *38* (1), 148–155.

(23) Jonker, M. T. O.; Hoenderboom, A. M.; Koelmans, A. A. Effects of sedimentary sootlike materials on bioaccumulation and sorption of polychlorinated biphenyls. *Environ. Toxicol. Chem.* **2004**, *23* (11), 2563–2570.

(24) Gallet, C.; Keller, C. Phenolic composition of soil solutions: comparative study of lysimeter and centrifuge waters. *Soil Biol. Biochem.* **1999**, *31* (8), 1151–1160.

(25) Haider, K.; Martin, J. P.; Filip, Z. *Humus Biochemistry*; Marcel Dekker, Inc.: New York, NY, 1975; Vol. 4, pp 195−244.

(26) Schweigert, N.; Hunziker, R. W.; Escher, B. I.; Eggen, R. I. L. Acute toxicity of (chloro-) catechols and (chloro-) catechol-copper combinations in Escherichia coli corresponds to their membrane toxicity in vitro. *Environ. Toxicol. Chem.* **2001**, *20* (2), 239–247.

(27) EPA. *Environmental Protection Agency, Sampling and Analysis Procedure for Screening of Priority Pollutants*; Cincinnati, USA, 1977.

(28) Pitois, A.; Abrahamsen, L. G.; Ivanov, P. I.; Bryan, N. D. Humic acid sorption onto a quartz sand surface: A kinetic study and insight into fractionation. *J. Colloid Interface Sci.* **2008**, *325* (1), 93–100.

(29) Greluk, M.; Hubicki, Z. Sorption of SPADNS azo dye on polystyrene anion exchangers: equilibrium and kinetic studies. *J. Hazard Mater.* **2009**, *172* (1), 289–297.

(30) Baldock, J. A.; Smernik, R. J. Chemical composition and bioavailability of thermally, altered *Pinus resinosa* (Red Pine) wood. *Org. Geochem.* **2002**, *33* (9), 1093–1109.

(31) Richard, D.; Nunez, M. D. D.; Schweich, D. Adsorption of complex phenolic compounds on active charcoal: Adsorption capacity and isotherms. *Chem. Eng. J.* **2009**, *148* (1), 1–7.

(32) Hoda, N.; Bayram, E.; Ayranci, E. , Removal of catechol and resorcinol from aqueous solution by adsorption onto high surface area activated carbon cloth. In *Innovations in Chemical Biology*; Springer: Netherlands: 2009; pp 213−223.

(33) Mukherjee, S.; Kumar, S.; Misra, A. K.; Fan, M. Removal of phenols from water environment by activated carbon, bagasse ash and wood charcoal. *Chem. Eng. J.* **2007**, *129* (1−3), 133–142.

(34) Brusseau, M. L.; Jessup, R. E.; Rao, P. S. C. Nonequilibrium sorption of organic chemicals: elucidation of rate-limiting processes. *Environ. Sci. Technol.* **1991**, *25* (1), 134–142.

(35) Pignatello, J. J.; Kwon, S.; Lu, Y. Effect of natural organic substances on the surface and adsorptive properties of environmental black carbon (char): Attenuation of surface activity by humic and fulvic acids. *Environ. Sci. Technol.* **2006**, *40* (24), 7757–7763.

(36) Zhou, M. L.; Martin, G.; Taha, S.; Sant'Anna, F. Adsorption isotherm comparison and modelling in liquid phase onto activated carbon. *Water Res.* **1998**, *32* (4), 1109–1118.

(37) Kleineidam, S.; Schuth, C.; Grathwohl, P. Solubility-normalized combined adsorption-partitioning sorption isotherms for organic pollutants. *Environ. Sci. Technol.* **2002**, *36* (21), 4689–4697.

(38) Bornemann, L. C.; Kookana, R. S.; Welp, G. Differential sorption behaviour of aromatic hydrocarbons on charcoals prepared at different temperatures from grass and wood. *Chemosphere* **2007**, *67* (5), 1033–1042.

(39) Chen, B.; Chen, Z. Sorption of naphthalene and 1-naphthol by biochars of orange peels with different pyrolytic temperatures. *Chemosphere* **2009**, *76* (1), 127–133.

(40) Chun, Y.; Sheng, G.; Chiou, C. T.; Xing, B. Compositions and sorptive properties of crop residue-derived chars. *Environ. Sci. Technol.* **2004**, *38* (17), 4649–4655.

(41) Allen-King, R. M.; Grathwohl, P.; Ball, W. P. New modeling paradigms for the sorption of hydrophobic organic chemicals to heterogeneous carbonaceous matter in soils, sediments, and rocks. *Adv. Water Resour.* **2002**, *25* (8−12), 985–1016.

(42) Zhou, Z.; Shi, D.; Qiu, Y.; Sheng, G. D. Sorptive domains of pine chars as probed by benzene and nitrobenzene. *Environ. Pollut.* **2010**, *158* (1), 201–206.

(43) Qiu, Y.; Xiao, X.; Cheng, H.; Zhou, Z.; Sheng, G. D. Influence of environmental factors on pesticide adsorption by black carbon: pH and model dissolved organic matter. *Environ. Sci. Technol.* **2009**, *43* (13), 4973–4978.

(44) Nguyen, T. H.; Ball, W. P. Absorption and adsorption of hydrophobic organic contaminants to diesel and hexane soot. *Environ. Sci. Technol.* **2006**, *40* (9), 2958–2964.

(45) Koelmans, A. A.; Meulman, B.; Meijer, T.; Jonker, M. T. O. Attenuation of polychlorinated biphenyl sorption to charcoal by humic acids. *Environ. Sci. Technol.* **2009**, *43* (3), 736–742.

Title: Catechol and humic acid sorption onto a range of laboratory-produced black carbons (biochars)

Authors: Kasozi, G. N.[1], A. R. Zimmerman[1*], P. Nkedi-Kizza[2], and B. Gao[3]

1. Department of Geological Sciences, University of Florida, 241 Williamson Hall, Gainesville, FL, 32611-2120

Phone: (352) 392-0070

e-mail: azimmer@ufl.edu

2. Department of Soil and Water Science, University of Florida, Gainesville, FL 32611

3. Department of Agricultural and Biological Engineering, University of Florida, Gainesville, FL 32611

*corresponding author and co-first author

21 pages

5 tables

11 figures

Surface area determination: Surface area was measured on a Quantachrome Autosorb1 using both N_2 (SA-N_2) and CO_2 (SA-CO_2) sorptometry on samples de-gassed under vacuum at least 24 h at 180 °C prior to analysis. SA-N_2 was calculated using BET theory on multi-point adsorption data from the 0.01-0.3 P/P_o linear segment of the N_2 adsorption isotherms at 77 K while CO_2 adsorption isotherms generated at 273 K in the <0.02 P/P_o range and were interpreted using canonical Monte Carlo simulations of the non-local density functional theory. Because N_2 is restricted from micropores (<1 nm *1*) and is further impeded by the stiffness of BC that likely occurs at 77 K, SA-N_2 represents nanopore-enclosed surfaces only. SA-CO_2 includes micropores because CO_2 diffusion is less kinetically limited and BC is more flexible at 273 K (*1, 2*) and has been found to be a more reliable indicator of BC microporosity (*2*).

Adsorption kinetics model descriptions: Catechol adsorption kinetics was examined using the pseudo-first order, pseudo-second order and diffusion models. The pseudo-first-order model, also known as the Lagergren first-order model followed Allen et al. (*3*) and is of the form:

$$\log(S_e - S_t) = \log S_{max} - \frac{k_1}{2.303}t$$

where S_e is the amount of catechol sorbed at equilibrium (mg kg^{-1}); S_t is the amount of catechol sorbed (mg kg^{-1}) at time t; k_1 is the equilibrium rate constant of first-order sorption (min^{-1}); S_{max} is the calculated adsorption capacity (mg kg^{-1}). Rate constants were obtained graphically plotting $\log(S_e - S_t)$ against t.

The linearized form of pseudo-second order kinetics model equation used was adapted from Donnaperna et al., (*4*) and Ho et al., (*5*):

$$S_t = S_e \frac{k_2 S_e t}{1 + k_2 S_e t}$$

where S_t (mg kg^{-1}) is the amount sorbed at any time t, S_e (mg kg^{-1}) is the equilibrium or maximum sorbed concentration, and k_2 is the apparent second order rate constant. Detailed model descriptions and derivations are available elsewhere (*4-7*).

Additional equilibrium adsorption model descriptions. Besides the Freundlich model described in the manuscript, three other adsorption isotherm models were examined: the Langmuir, the Langmuir-Freundlich hybrid, and the Toth model. Adsorption data were fit to the Freundlich model graphically using its linearized form:

$$\ln(S_e) = \ln(K_f) + n\ln(C_e)$$

where S_e is the sorbed concentration (mg kg^{-1}), C_e is the equilibrium sorbate concentration (mg L^{-1}), K_f, is the Freundlich affinity coefficient (mg$^{(1-n)}$ L^n kg^{-1}) and n, the Freundlich linearity parameter.

The Langmuir adsorption model assumes both a finite number of identical adsorption sites (a monolayer) and no interaction between sorbate molecules on the sorbent surface. The data was fit to the model graphically using the linearized equation form:

$$\frac{C_e}{S_e} = \frac{C_e}{S_{max}} + \frac{1}{S_{max} * K_L}$$

where S_e is the sorbed equilibrium concentration (mg kg^{-1}), K_L is the Langmuir constant, representing the free energy of adsorption (strength of sorbate-sorbent interaction), S_{max} is the monolayer adsorption capacity (mg kg^{-1}) and C_e is the solution concentration at equilibrium (mg L^{-1}).

The Langmuir-Freundlich model is a hybrid of the Freundlich and Langmuir models. The equation used to fit the data in this study, has been previously used in other studies (*4, 8, 9*) and is described as:

$$S_e = \frac{S_{max}K_{LF}C_e^{a_{LF}}}{1 + (K_{LF}C_e)^{a_{LF}}}$$

where S_e is the sorbed equilibrium concentration (mg kg^{-1}), K_{LF} is the Langmuir-Freundlich constant, Q_{max} is the maximum adsorbed concentration (mg kg^{-1}), C_e is the equilibrium solution concentration (mg L^{-1}) and a_{LF} is the heterogeneity index.

Following previous studies (*10, 11*), the Toth adsorption isotherm equation was of the form:

$$Se = \frac{S_{max}K_TC_e}{(1 + (K_TC_e)^t)^{1/t}}$$

where K_T and t are constants. The parameter t is related to the surface heterogeneity, when $t = 1$, the Toth equation reduces to Langmuir equation. The Langmuir-Freundlich and Toth equations were fit to the data using a progressive least-squares minimization approach.

Statistical analyses. The success of each kinetic or adsorption model was evaluated using two goodness of fit statistics, the coefficient of determination (R^2) and the mean relative deviation modulus ($P*$). The coefficient of determination was of the form:

$$R^2 = 1 - \frac{SS_{err}}{SS_{tot}}$$

where SS_{err} is the sum of squares of the differences between the observed (S_{t_obs}) and model-predicted (S_t*) adsorption for a given concentration and SS_{tot} is the sum of squares of the differences between each observed and mean observed data value. The equation for the mean relative deviation modulus (*12, 13*) was of the form:

$$P* = \frac{100}{n}\left[\frac{|S_{t\_obs} - S_t*|}{S_{t\_obs}}\right]$$

where n = number of observations. A model is considered acceptable if it has a $P*$ less than 10.

Analysis of variance (ANOVA) for independent samples was carried out to test for differences in the goodness of fit among the different isotherm models. Tukey's honest significant difference (HSD) pair-wise comparison was used to test for significance ($\alpha = 0.05$) using SAS version 9.2 (*14*).

Table S1. Properties of studied laboratory-made biochars

Biochar type	C%	SA-N_2 (m^{2}g^{-1})	SA-CO_2 (m^{2}g^{-1})	VM%	Ash%
Coarse					
Oak-250cs	55.2	1	331	66	1.4
Oak-400cs	69.6	2	252	52	2.6
Oak-650cs	78.8	225	528	21	3.7
Pine-250cs	58.0	0	373	61	0.3
Pine-400cs	68.6	3	361	59	0.5
Pine-650cs	83.0	285	643	25	1.0
Grass-250cs	52.7	3	221	62	6.8
Grass-400cs	58.6	6	164	51	13.2
Grass-650cs	63.8	77	427	33	15.8
Coarse Aged					
Oak-250a	57.1	2	291	63	1.3
Oak-400a	69.3	3	225	56	2.2
Oak-650a	80.5	166	539	44	2.9
Pine-250a	63.0	2	286	50	0.4
Pine-400a	68.0	5	324	20	0.2
Pine-650a	81.0	59	594	24	0.5
Grass-250a	52.5	3	281	63	4.1
Grass-400a	64.4	2	210	53	3.6
Grass-650a	72.0	261	476	25	7.9

NOTES: cs = coarse, a = aged (leached), C% = weight percent organic carbon; SA-N_2 and SA-CO_2= surface area determined by N_2 and CO_2 sorptometry, respectively; VM% = weight percent volatile matter; Ash% = weight percent inorganic.

Table S2. Model parameters and goodness of fit statistics for the two kinetic models tested

Biochar	Diffusion				Pseudo 2nd order			
Type	K_i	C	R^2	$P*$	K_2	S_e	R^2	$P*$
Catechol Sorption								
Oak-400fn	1500	1.1×10^4	0.91	4.7	1.1×10^{-4}	18103	0.81	34.84
Oak-400cs	1390	6.2×10^3	0.85	8.55	9.1×10^{-5}	12837	0.61	45.59
Oak-650fn	6860	1.5×10^4	0.91	12.36	3.5×10^{-5}	42553	0.65	27.72
Oak-650cs	5330	1.5×10^4	0.89	11.38	5.3×10^{-5}	36101	0.58	25.29
Grass-400fn	5410	1.2×10^4	0.97	4.92	2.2×10^{-5}	37594	-0.07	42.92
Grass-400cs	2490	1.1×10^4	0.84	8.66	1.3×10^{-4}	20492	-0.67	30.02
Grass-650fn	7359	3.6×10^4	0.85	10.08	4.8×10^{-5}	66534	0.99	23.65
Grass-650cs	8380	2.6×10^4	0.88	11.33	2.1×10^{-5}	62112	0.59	22.74
Humic Acid Sorption								
Oak-400a	-	-	-	-	4.6×10^{-3}	4237	0.77	-
Oak-650a	-	-	-	-	2.7×10^{-3}	4694	0.75	-
Grass-400a	-	-	-	-	4.3×10^{-3}	4098	0.66	-
Grass-650a	-	-	-	-	4.5×10^{-3}	6098	0.45	-

NOTES: cs = coarse, fn = fine a = aged; K_i = diffusion rate constant (mg kg^{-1} d$^{-1/2}$); C = intercept; K_2 = Pseudo-second order constant (kg mg^{-1} d^{-1}); S_e = Equilibrium sorbed concentration (mg kg^{-1}); R^2= Coefficient of determination; $P*$ = normalized percent deviation.

Table S3. Langmuir-Freundlich, Toth and Langmuir model parameters

Biochar Type	Langmuir-Freundlich			Toth			Langmuir	
	$S_{LF\,max}$	K_{LF}	a_{LF}	S_{Tmax}	K_T	t	S_{Lmax}	K_L
Coarse Biochar								
Oak-250cs	9.8×10^3	3.5×10^{-01}	1.00	1.4×10^4	1.1×10^3	0.19	1.0×10^4	0.83
Oak-250cs	3.2×10^4	1.8×10^{-02}	0.83	2.3×10^{11}	1.1×10^{10}	0.02	2.5×10^4	0.01
Oak-400cs	6.9×10^4	1.7×10^{-01}	0.33	2.2×10^5	2.0×10^4	0.10	5.0×10^4	0.04
Oak-650cs	2.9×10^4	4.7×10^{-02}	0.46	1.0×10^{11}	1.8×10^{10}	0.02	1.2×10^4	0.03
Pine-250cs	2.5×10^4	6.9×10^{-03}	0.78	1.6×10^{16}	2.1×10^{16}	0.01	1.4×10^4	0.01
Pine-400cs	1.9×10^9	1.5×10^{-06}	0.26	3.3×10^5	3.7×10^4	0.08	1.4×10^4	0.02
Pine-650cs	2.7×10^8	2.6×10^{-05}	0.10	1.3×10^4	7.1×10^{-2}	1.00	1.2×10^4	0.12
Grass-250cs	8.1×10^4	3.6×10^{-02}	0.52	1.4×10^{11}	2.1×10^{10}	0.03	4.0×10^4	0.02
Grass-400cs	7.6×10^8	3.6×10^{-05}	0.17	4.1×10^4	2.7×10^5	0.11	8.3×10^4	0.06
Coarse –Aged Biochar								
Oak-250a	3.1×10^8	1.1×10^{-05}	0.26	5.4×10^8	1.7×10^8	0.03	1.7×10^4	0.03
Oak-400a	1.8×10^5	3.5×10^{-03}	0.59	9.9×10^5	8.0×10^{14}	0.02	2.5×10^4	0.01
Oak-650a	1.0×10^9	7.1×10^{-06}	0.25	5.6×10^5	1.4×10^5	0.08	3.6×10^4	0.03
Pine-250a	1.3×10^5	3.3×10^{-02}	0.31	4.2×10^5	9.3×10^4	0.08	2.5×10^4	0.03
Pine-400a	2.8×10^4	8.1×10^{-03}	0.72	4.3×10^{16}	3.4×10^{15}	0.01	1.4×10^4	0.01
Pine-650a	7.5×10^8	3.9×10^{-06}	0.30	7.1×10^6	8.7×10^{05}	0.05	2.0×10^4	0.02
Grass-250a	1.2×10^7	5.4×10^{-04}	0.14	4.8×10^4	5.0×10^{05}	0.11	1.6×10^4	0.04
Grass-400a	1.1×10^5	4.5×10^{-03}	0.65	6.2×10^{14}	3.3×10^{12}	0.02	3.3×10^4	0.01
Grass-650a	4.3×10^5	4.6×10^{-02}	0.20	2.4×10^5	1.4×10^4	0.11	5.0×10^4	0.05
Fine Biochar								
Oak-250fn	3.1×10^8	1.1×10^{-05}	0.26	8.7×10^5	1.5×10^1	0.12	2.5×10^4	0.01
Oak-400fn	1.7×10^8	3.5×10^{-03}	0.59	5.8×10^9	1.6×10^8	0.03	3.3×10^4	0.02
Oak-650fn	1.7×10^8	7.1×10^{-06}	0.25	8.0×10^7	1.4×10^6	0.05	1.0×10^5	0.01
Pine-250fn	2.0×10^9	3.3×10^{-02}	0.31	3.1×10^6	3.6×10^5	0.06	1.4×10^4	0.03
Pine-400fn	1.9×10^9	8.1×10^{-03}	0.72	6.0×10^{17}	5.1×10^{16}	0.01	2.0×10^4	0.01
Pine-650fn	4.1×10^9	3.9×10^{-06}	0.30	1.8×10^5	2.3×10^4	0.10	2.5×10^4	0.03

NOTES: cs = coarse, a = aged, fn = fine, S_{LFmax} = Langmuir-Freundlich (LF)

Maximum adsorption capacity, K_{LF} = the LF binding affinity, a_{LF} = LF homogeneity index, S_{max} = Toth model observed maximum sorption capacity, K_T = the Toth binding affinity, t = homogeneity index S_{Lmax} = calculated Langmuir sorption maxima, K_L = Langmuir sorption constant.

Table S4. Goodness of fit parameters for Freundlich, Langmuir-Freundlich, Toth and Langmuir models fitting catechol sorption onto biochar data.

Biochar	Freundlich		LF		Toth		Langmuir	
Type	R^2	$P*$	R^2	$P*$	R^2	$P*$	R^2	$P*$
Coarse Biochar								
Oak-250cs	0.49	15.94	0.67	11.11	0.53	14.76	0.44	17.65
Oak-400cs	0.92	10.09	0.96	12.90	0.92	23.26	0.94	15.12
Oak-650cs	0.97	4.37	0.98	3.40	0.98	3.54	0.27	27.48
Pine-250cs	0.86	22.22	0.87	24.18	0.86	26.04	0.83	34.14
Pine-400cs	0.99	6.37	0.99	7.62	0.80	40.15	0.98	14.77
Pine-650cs	0.95	6.53	0.95	6.95	0.94	7.14	0.70	23.98
Grass-250cs	0.31	12.60	0.31	12.70	0.43	10.70	0.12	12.37
Grass-400cs	0.95	12.85	0.96	15.28	0.95	13.60	0.92	25.37
Grass-650cs	0.94	9.85	0.94	10.35	0.93	11.93	0.74	24.38
Coarse –Aged Biochar								
Oak-250a	0.96	15.98	0.92	15.57	0.74	18.45	0.67	33.53
Oak-400a	0.98	9.20	0.94	9.16	0.85	35.69	0.94	23.27
Oak-650a	0.89	16.21	0.89	16.30	0.85	15.48	0.72	33.10
Pine-250a	0.98	6.48	0.98	6.01	0.96	7.30	0.63	29.80
Pine-400a	0.96	8.49	0.98	8.60	0.82	42.36	0.97	17.62
Pine-650a	0.97	6.31	0.97	6.31	0.97	6.64	0.84	22.99
Grass-250a	0.95	4.50	0.95	4.21	0.94	3.88	0.01	19.19
Grass-400a	1.00	3.87	1.00	4.25	0.82	30.08	0.93	20.08
Grass-650a	0.99	3.24	0.99	3.03	0.99	3.17	0.65	29.08
Fine Biochar								
Oak-250fn	0.78	27.95	-	-	0.89	29.69	0.65	37.50
Oak-400fn	0.98	5.11	0.98	5.23	0.96	8.33	0.90	20.39
Oak-650fn	0.97	4.33	0.97	4.35	0.97	4.69	0.29	28.26
Pine-250fn	0.97	6.85	0.97	7.61	0.96	6.79	0.80	27.58
Pine-400fn	0.99	5.93	0.99	6.79	0.71	41.49	0.95	14.03
Pine-650fn	0.98	3.41	0.98	3.67	0.97	4.52	0.65	23.98

NOTES: LF = Langmuir-Freundlich, R^2 = coefficient of determination, $P*$ = normalized percent deviation.

Table S5. Data summary statistics for comparisons of coefficients of determination (R^2) for each sorption model using general linear ANOVA model.

Model	Mean R^2	N
Langmuir-Freundlich	0.92[a]	23
Freundlich	0.90[a]	24
Toth	0.86[a]	24
Langmuir	0.69	24

NOTES: 'a' signifies means that are not significantly different.
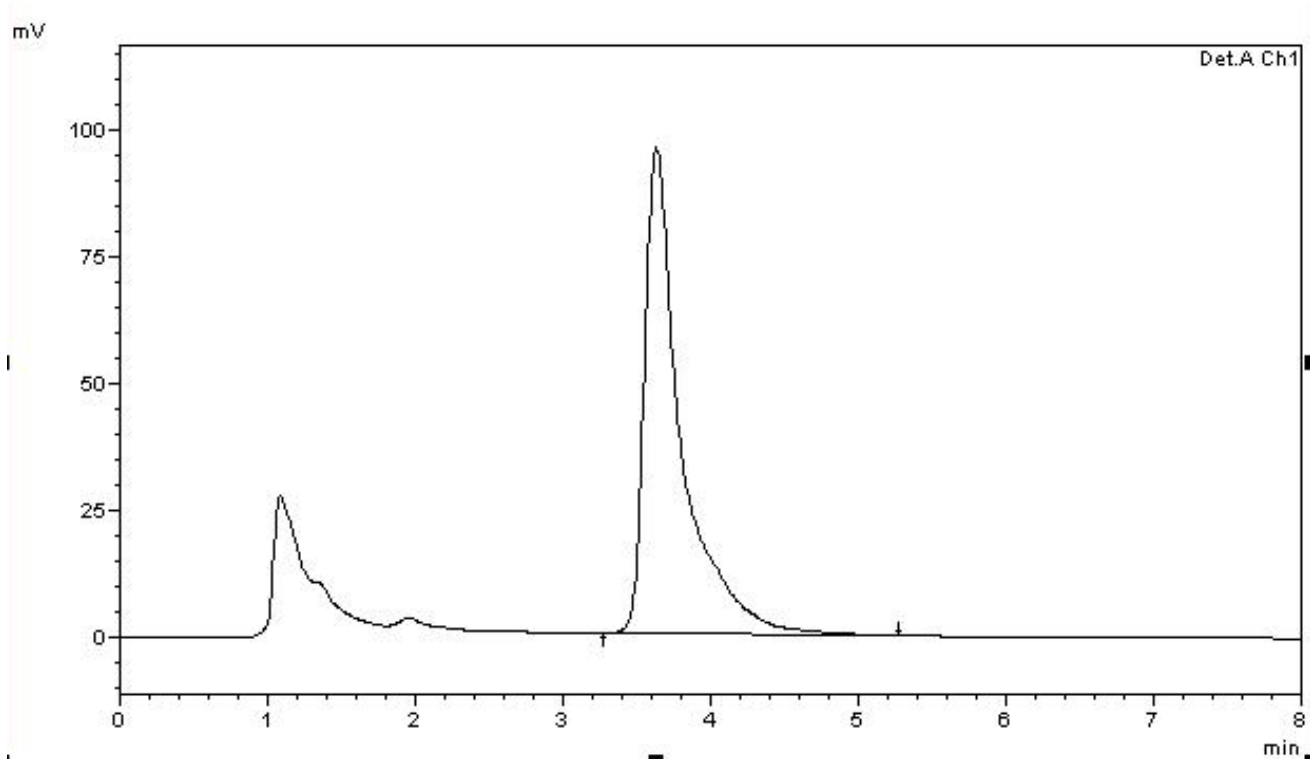
Figure S1. Representative HPLC chromatogram of supernatant following a period of catechol sorption to Oak-400 biochar. Shows release of dissolved organic matter from the biochar (leachate: 1-2 min retention time) separated from catechol peak (3.2-5 min) and the absence of additional peaks indicative of catechol degradation products.
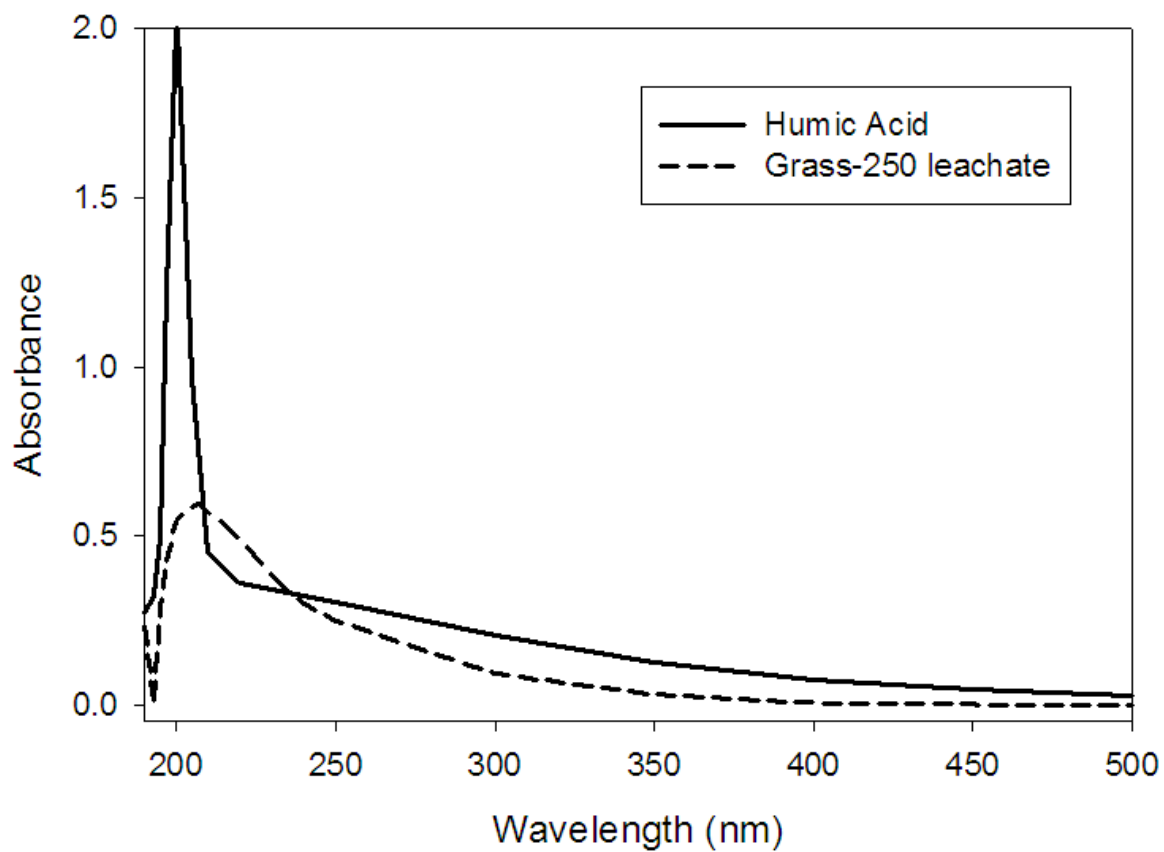
Figure S2. Representative UV spectra showing the spectraphotometric similarity between biochar leachate (Grass-250 ^{o}C) and humic acid.
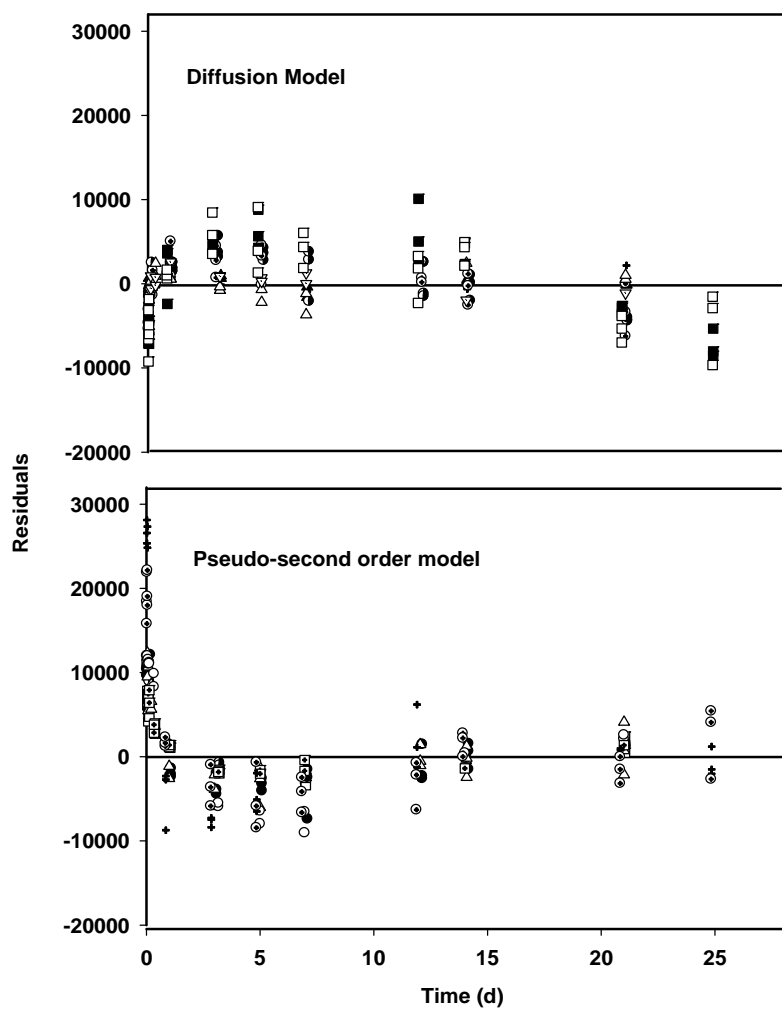
Figure S3. Residual plots for catechol adsorption kinetics model fits for a) Diffusion model and b) Pseudo-second order kinetics model. The lack of structure in the diffusion model compared to the pseudo-second order model residuals indicate that the former is a better simulation of the data.
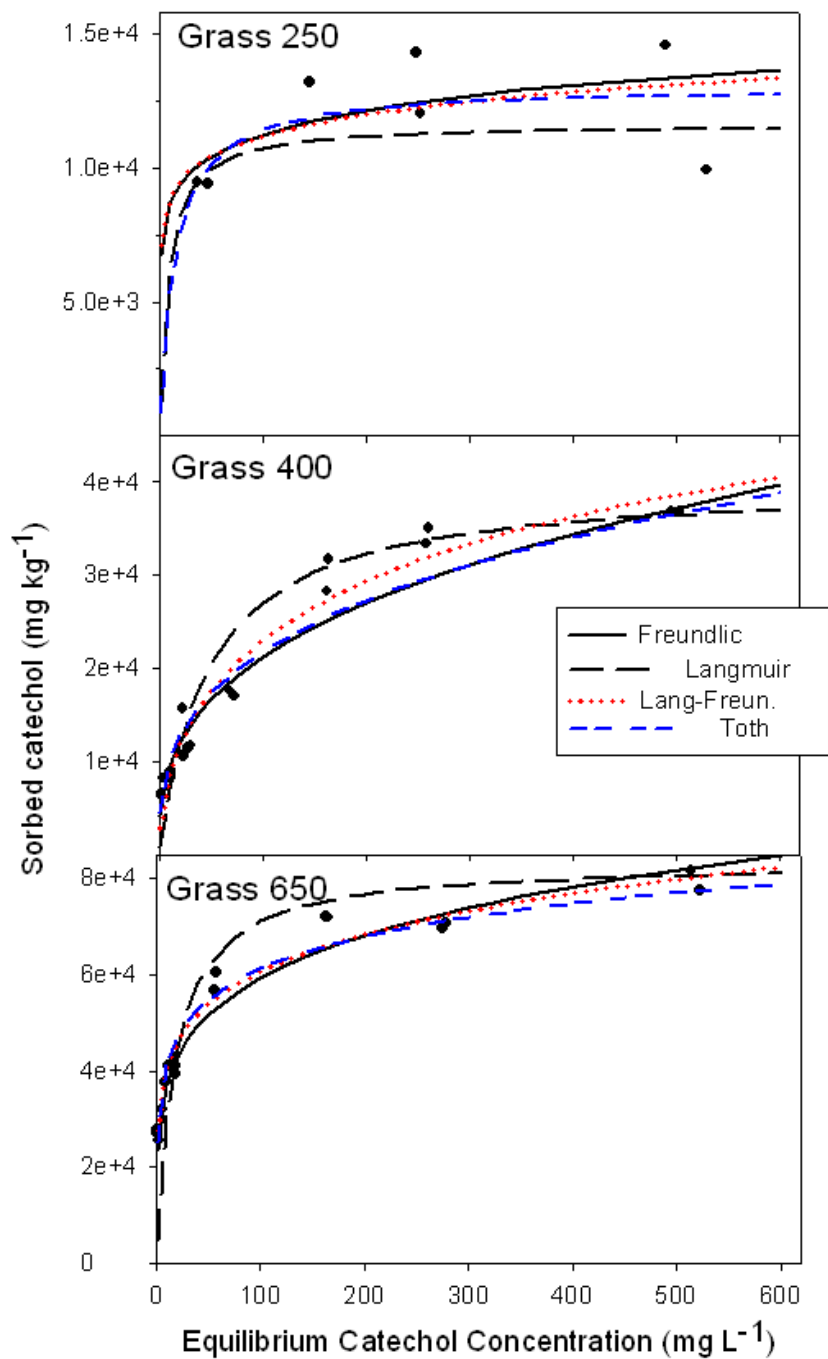
Figure S4. Comparison of sorption isotherm models for catechol onto coarse grass biochar (250, 400 and 650 °C) using Freundlich, Langmuir, Langmuir-Freundlich hybrid and Toth adsorption isotherm models.
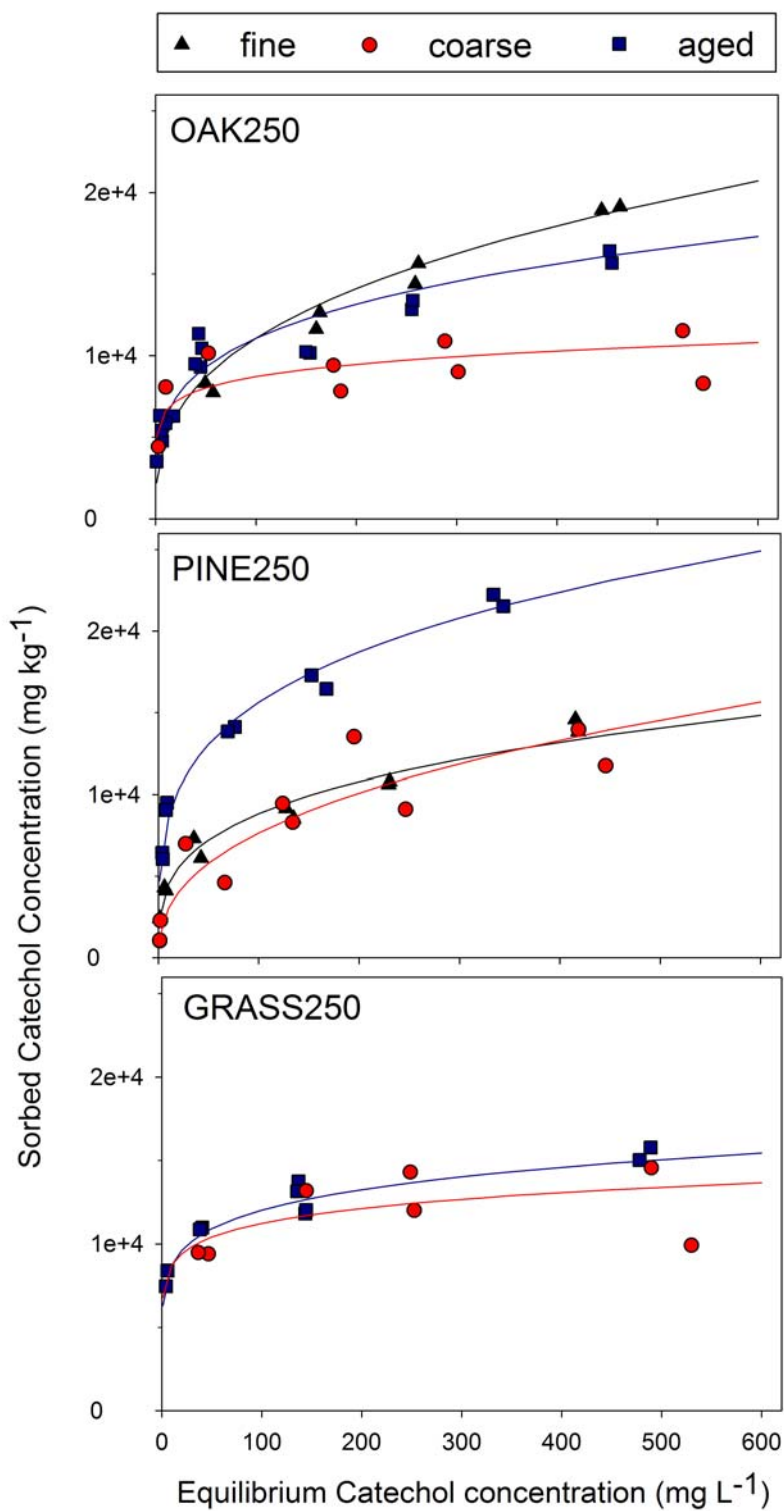
Figure S5. Catechol sorption isotherms for oak, pine and grass (coarse, fine and aged) combusted at 250°C. Data modeled using Freundlich model (solid lines).
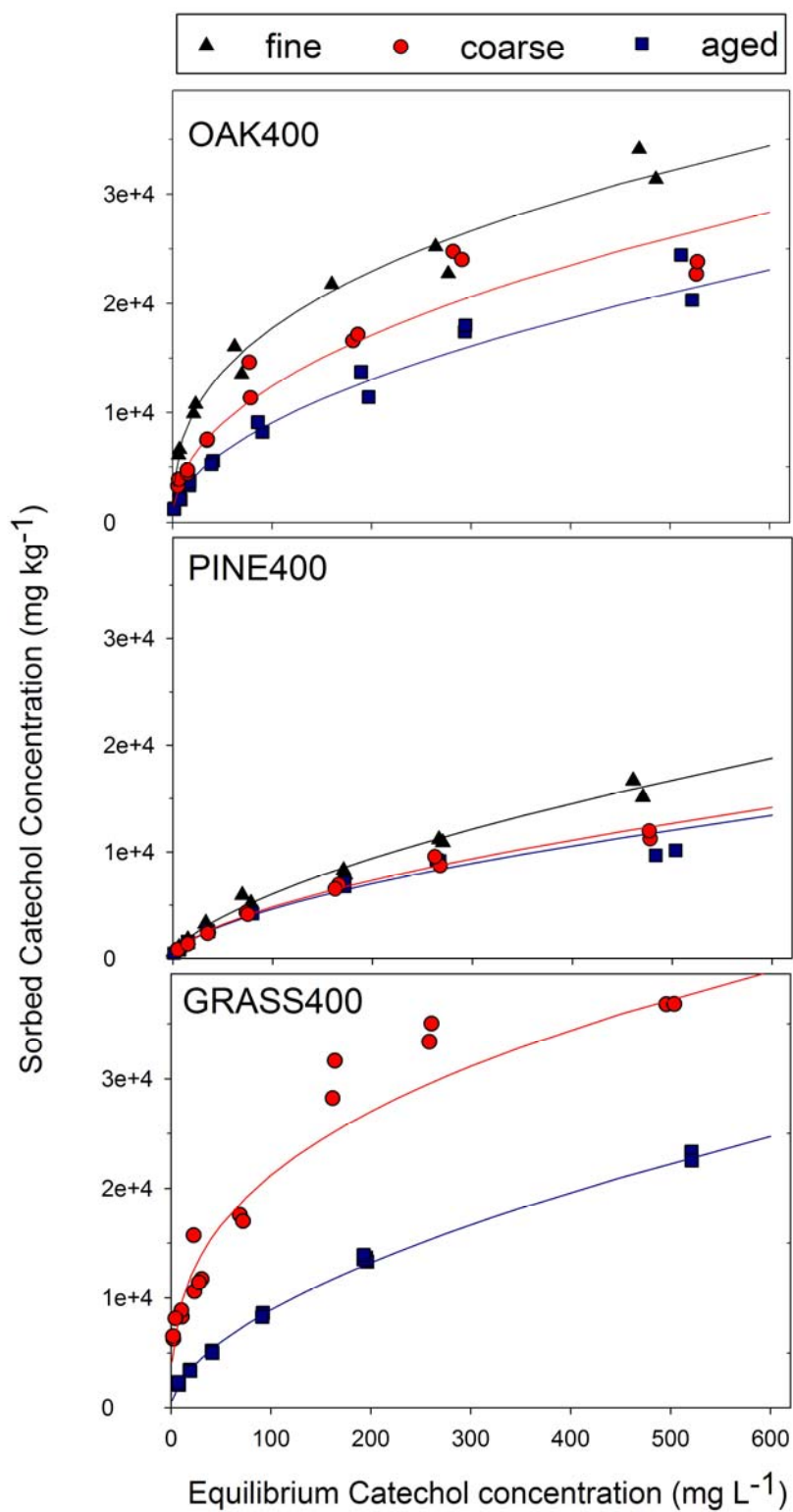
Figure S6. Catechol sorption isotherms for oak, pine and grass (coarse, fine and aged) pyrolyzed at 400°C. Data modeled using Freundlich model (solid lines).
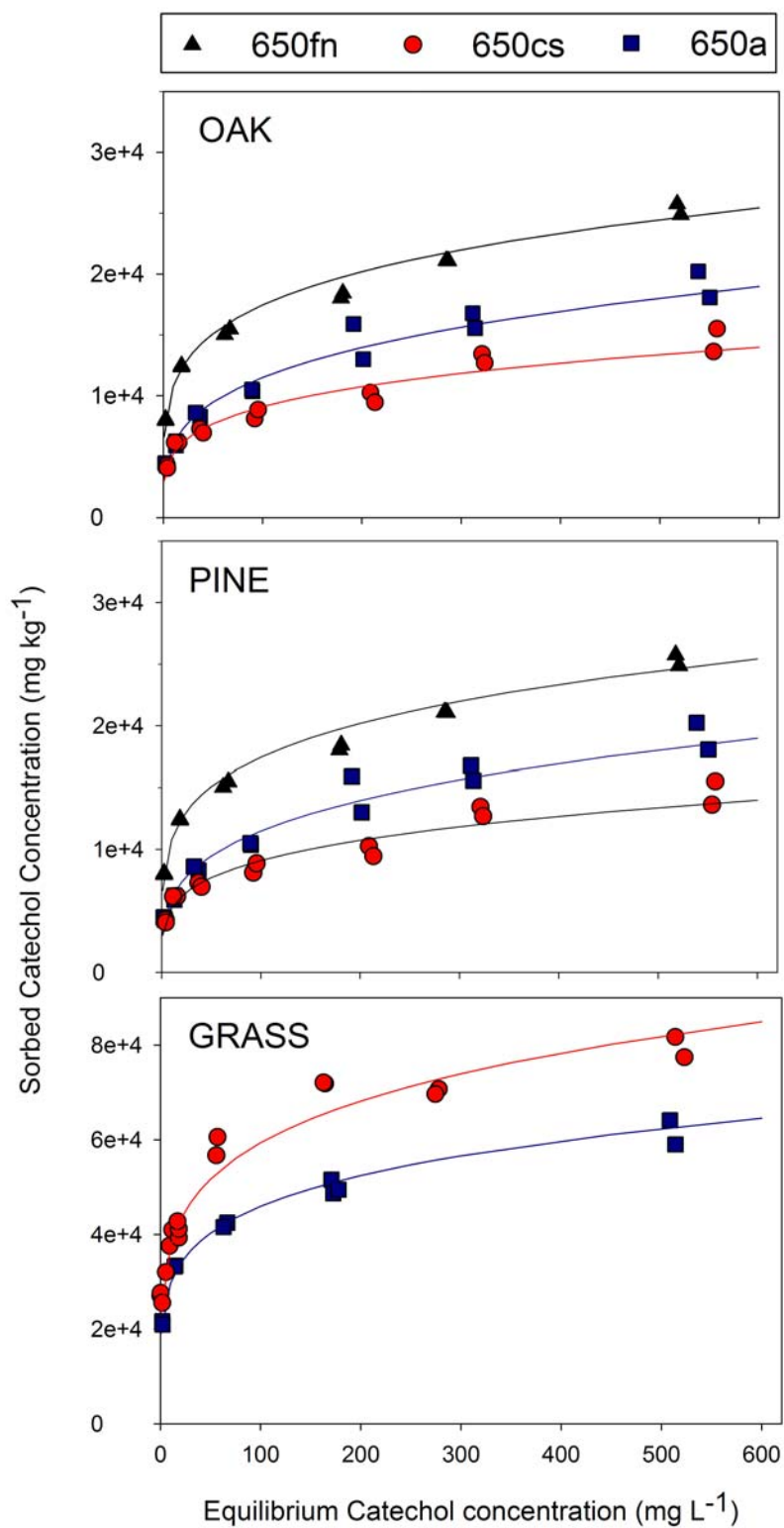
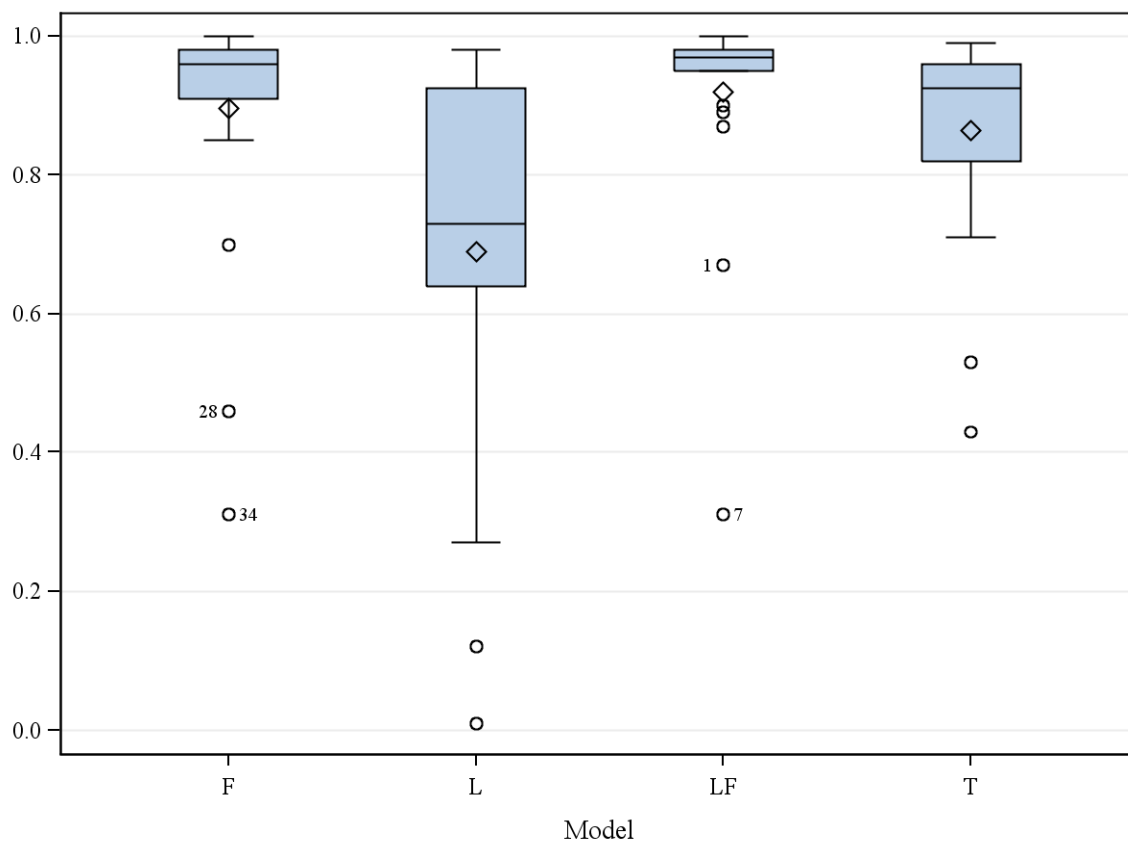Figure S7. Catechol sorption isotherms for oak, pine and grass (coarse, fine and aged) pyrolyzed at 650°C. Data modeled using Freundlich model (solid lines).

Figure S8. Boxplot showing the distribution of the coefficients of determination for goodness of fit for all catechol sorption isotherms. F = Freundlich; L = Langmuir; LF = Langmuir-Freundlich hybrid model and T = Toth model.
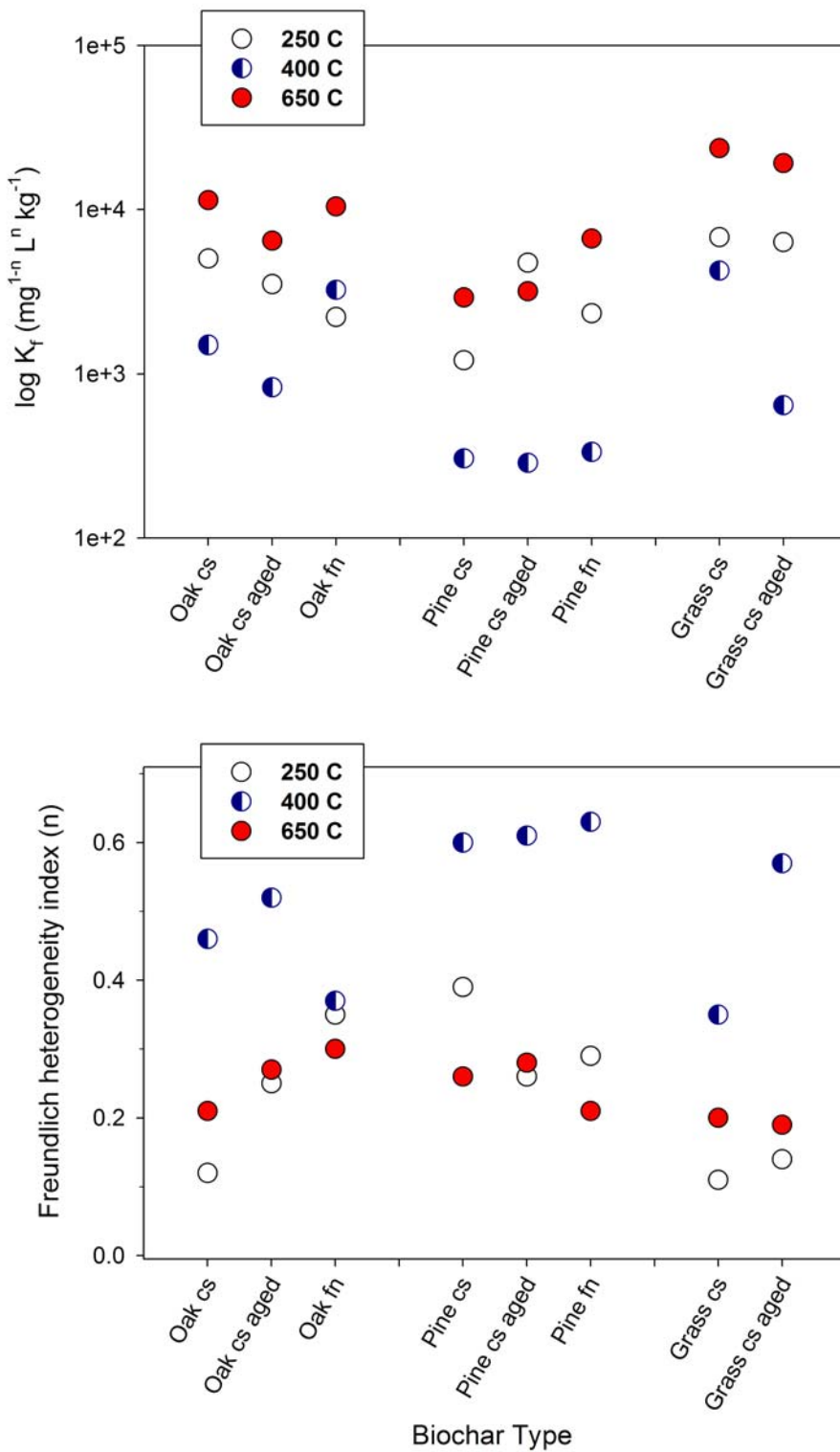
Figure S9. Freundlich coefficient (K_f) and surface heterogeneity index (n) for catechol sorption to Oak, Pine and Grass biochar (cs = coarse, fn = fine, aged = leached).
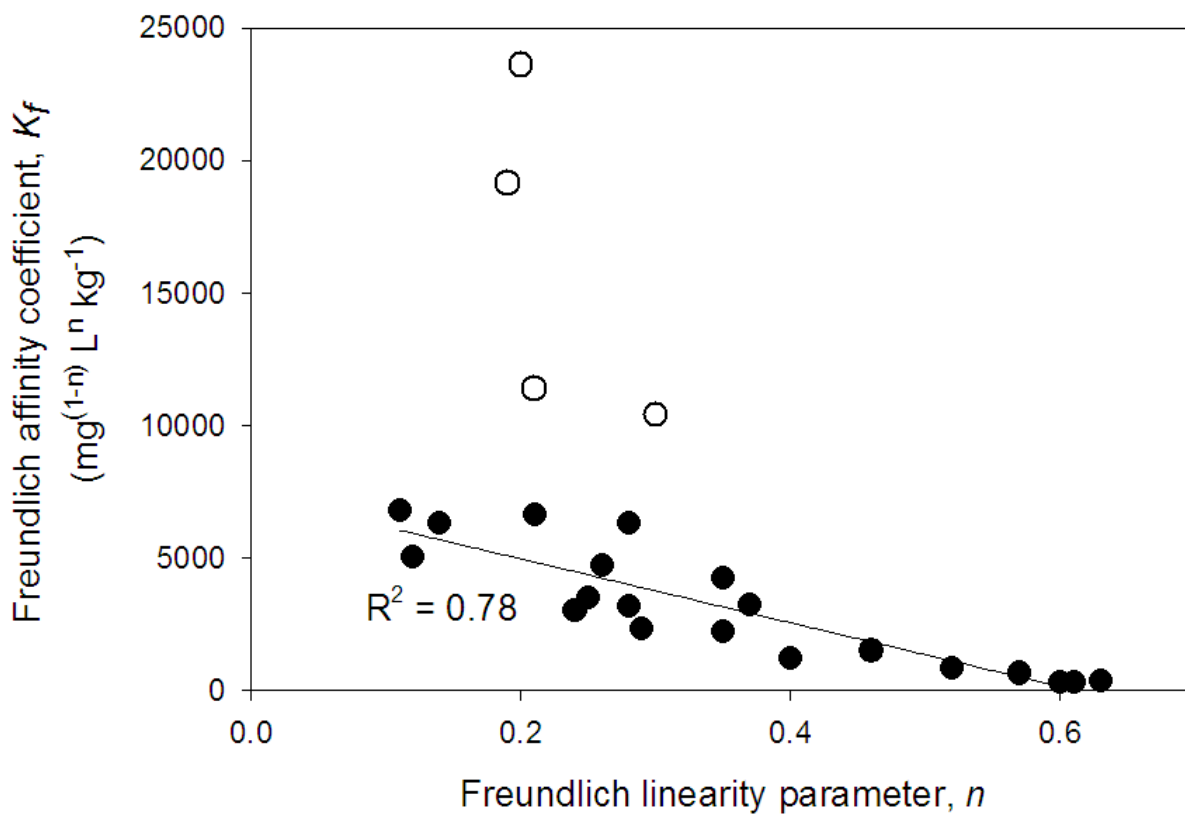
Figure S10. Linear relationship between *n,* the Freundlich linearity parameter and the Freundlich affinity coefficient ($mg^{(1-n)} L^n kg^{-1}$) of the sorbate catechol on all biochars (solid circles) excluding the biochars: Oak-650-coarse, Oak-650-fine, Oak-650-aged and Grass-650-coarse (open circles).
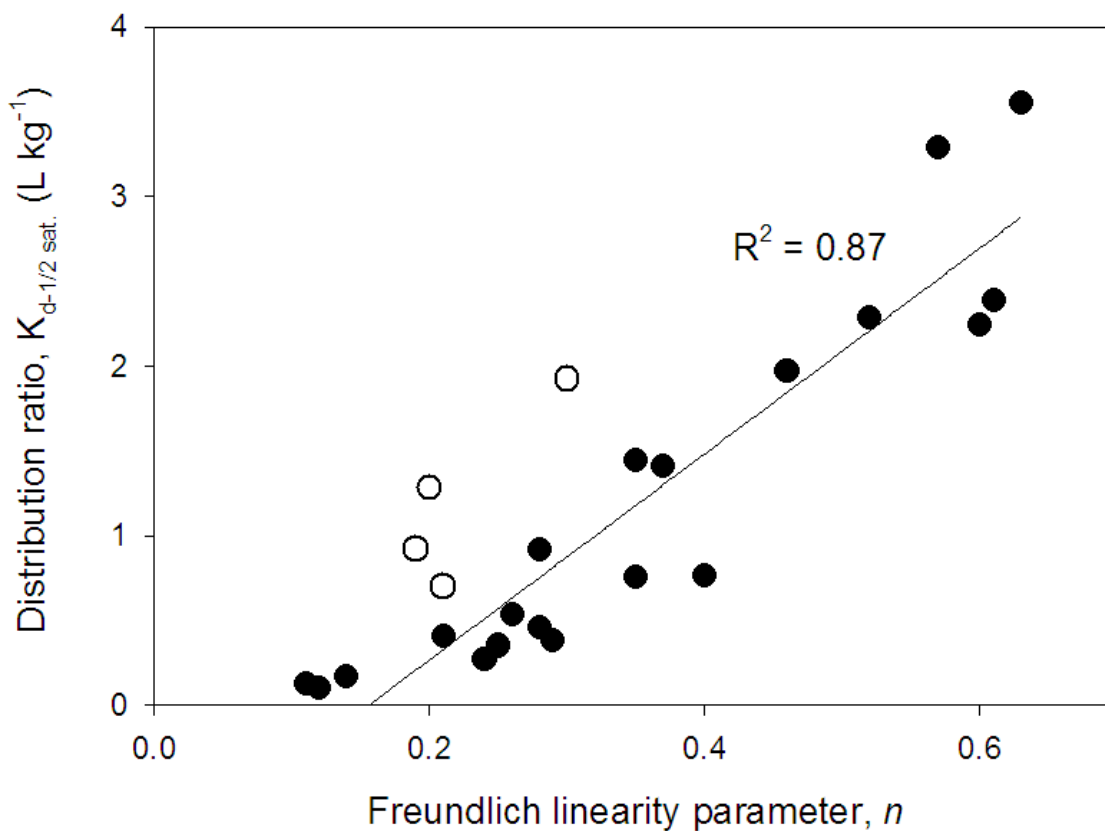
Figure S11. Linear relationship between *n,* the Freundlich linearity parameter and the solid-water distribution ratio, K_d (L kg^{-1}) at one-half the saturation concentration of the sorbate catechol on all biochars (solid circles) excluding the biochars: Oak-650-coarse, Oak-650-fine, Oak-650-aged and Grass-650-coarse (open circles).

References Cited in Supplementary Information Section

(1) de Jonge, H.; de Jonge, L.W.; Mittelmeijer-Hazeleger, M.C. The microporous structure of organic and mineral soil materials. *Soil Sci.* **2000,** 165 (2), 99-108.

(2) Pignatello, J.J.; Kwon, S.; Lu, Y. Effect of natural organic substances on the surface and adsorptive properties of environmental black carbon (char): Attenuation of surface activity by humic and fulvic acids. *Environ. Sci. Technol.* **2006,** 40 (24), 7757-7763.

(3) Allen, S.J.; Koumanova, B.; Kircheva, Z.; Nenkova, S. Adsorption of 2-nitrophenol by technical hydrolysis lignin: Kinetics, mass transfer, and equilibrium studies. *Ind. Eng. Chem. Res.* **2005,** 44 (7), 2281-2287.

(4) Donnaperna, L.; Duclaux, L.; Gadiou, R.; Hirn, M.P.; Merli, C.; Pietrelli, L. Comparison of adsorption of Remazol Black B and Acidol Red on microporous activated carbon felt. *J. Colloid Interface Sci.* **2009,** 339 (2), 275-284.

(5) Ho, Y.S.; McKay, G. Pseudo-second order model for sorption processes. *Process Biochem.* **1999,** 34 (5), 451-465.

(6) Greluk, M.; Hubicki, Z. Sorption of SPADNS azo dye on polystyrene anion exchangers: equilibrium and kinetic studies. *J Hazard Mater* **2009,** 172 (1).

(7) Srihari, V.; Babu, S.M.; Ashutosh, D. Kinetics of phenol-sorption by raw agro-wastes. *Journal of Applied Sciences* **2006,** 6 (1).

(8) Umpleby, R.J.; Baxter, S.C.; Chen, Y.Z.; Shah, R.N.; Shimizu, K.D. Characterization of molecularly imprinted polymers with the Langmuir-Freundlich isotherm. *Analytical Chemistry* **2001,** 73 (19), 4584-4591.

(9) Zimmerman, A.R.; Goyne, K.W.; Chorover, J.; Komarneni, S.; Brantley, S.L. Mineral mesopore effects on nitrogenous organic matter adsorption. *Org. Geochem.* **2004,** 35 (3), 355-375.

(10) Pikaar, I.; Koelmans, A.A.; van Noort, P.C.M. Sorption of organic compounds to activated carbons. Evaluation of isotherm models. *Chemosphere* **2006,** 65 (11), 2343-2351.

(11) Richard, D.; Nunez, M.D.D.; Schweich, D. Adsorption of complex phenolic compounds on active charcoal: Adsorption capacity and isotherms. *Chem. Eng. J.* **2009,** 148 (1), 1-7.

(12) Chen, C.C. Moisture sorption isotherms of pea seeds. *J. Food Eng.* **2003,** 58 (1), 45-51.

(13) Hoda, N.; Bayram, E.; Ayranci, E., Removal of catechol and resorcinol from aqueous solution by adsorption onto high surface area activated carbon cloth. In *Innovations in Chemical Biology*, Springer Netherlands: 2009; pp 213-223.

(14) SAS; Institute *SAS*, 9.2; Cary, NC, 2002.